

An experimental study of natural convection with coupled heat and mass transfer in porous media

J. SHERIDAN and A. WILLIAMS

Department of Mechanical Engineering, Monash University, Clayton, Victoria, 3168, Australia

and

D. J. CLOSE

Department of Mechanical Engineering, James Cook University, Townsville, Queensland, 4811, Australia

(Received 28 August 1990 and in final form 6 September 1991)

Abstract—This paper examines coupled heat and mass transfer in porous media where natural convection is caused by temperature and concentration differences. Two alternative non-dimensional models are developed and used to correlate the experimentally measured heat transfer across a porous medium. It is shown that a parametric model correlates the data well with a general form, $Nu \propto (Ra Da N)^{0.295} Ja^{-0.45}$. The other model, based on the analogy between heat and mass transfer, is less accurate in predicting heat transfer but the results are good enough to suggest that such analogy models could be used in a wide range of heat and mass transfer processes. The effect of bed geometry on the two models is also discussed.

1. INTRODUCTION

NATURAL convection of a gas in a packed bed with simultaneous evaporation and condensation of a vapour has been proposed by Close and Peck [1] as a method of providing high effective thermal conductances in thermal energy stores. The physical requirements for the process are as shown in Fig. 1. A vessel containing a packed bed initially has a gas (for example, air) in the voids. A shallow layer of liquid (for example, water) in the base of the container is heated forming a vapour, and the gas and vapour mixture convects through the packing.

The authors believe there are many potential applications for this process either in naturally occurring situations, such as in wet fibrous insulation, or in the engineering design of thermal stores, building components or electronic cooling devices. This study provides basic information for the analysis of such systems. The potential of the process can be gauged from the following.

1. The addition of water in the air/water combination results in an increase in the heat transferred which is negligible at temperatures around 20°C but can be several orders of magnitude at 90°C.

2. Because the change in heat transfer is caused both by buoyancy and latent heat effects, there is potential, yet to be examined, for controlling the heat transfer by varying the operating temperature and the gas and vapour used. Buoyancy, and consequently the flow pattern, depends on the difference in molecular weights between the gas and the vapour and the level of concentration of the vapour, as determined by the

dependence of the vapour pressure on temperature. Hence, with the appropriate choice of components the natural convection can be increased or decreased as a function of the temperature level. Close and Sheridan [2] have discussed the situation where buoyancy reverses for a mixture of ethanol and air in an open cavity. At such a 'neutral buoyancy' point there is a reduction in the heat transferred. By the appropriate choice of inert gas and volatile component(s) the heat and fluid flow of a component or system could thus be controlled passively.

A theoretical basis was established by Close [3], who showed that with certain assumptions an analogy could be formed with the simple case of a single fluid. The most important of these assumptions was that of infinite rate coefficients between the fluid and adjacent solid, leading to the conclusion that the gas/vapour mixture is saturated everywhere. Data for four gas mixtures convecting in a bed of glass spheres, as described by Close and Peck [4], showed the usefulness of the theory but raised questions about some of the assumptions.

An extension to the theory was made by Sheridan and Close [5], where the data of Close and Peck [4] were further analysed using an extended range of parameters. While the conclusions drawn were useful they were limited by the restricted data set.

In this paper, experimental results are presented using the two different models. These models, which are briefly described below, were developed for two main purposes.

1. To predict the behaviour of a porous medium or

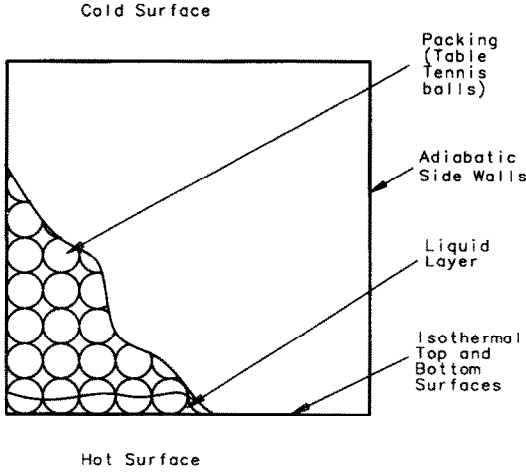


FIG. 1. Schematic of the physical model.

culties in writing the equations in their most complete form. These difficulties are not insurmountable, however, and the final form of the equations derived are the same as those derived by a more rigorous method.

2.1. Conservation equations

In general (see Bird *et al.* [6] or Slattery [7]) for a mixture of i components the conservation equations can be written in general form as follows.

Mass :

$$\frac{\partial \rho_i}{\partial t} + \nabla \cdot (\rho_i \mathbf{v}_i) = r_i \quad (1)$$

Momentum (Darcy's Law) :

$$\mathbf{v}_i = -\frac{\kappa}{\mu} (\nabla p - \rho_i \mathbf{g}) \quad (2)$$

where it has been assumed that the tensor κ can be written as a scalar because the bed is isotropic and homogeneous.

Energy :

$$\frac{\partial (\rho_i h_i)}{\partial t} + \nabla \cdot (\rho_i h_i \mathbf{v}_i) = -\nabla \cdot \mathbf{q}_i - \frac{Dp}{Dt} - \tau : (\nabla \mathbf{v}_i) + \dot{Q}_i \quad (3)$$

where D/Dt is the material derivative. These were applied to all phases involved in the process, i.e. solid, liquid, vapour and gas. Further details of the development have been presented by Sheridan [8]. However, points worth noting are presented below.

1. The momentum equation for the gas/vapour mixture was written as a single equation in terms of \mathbf{v}_γ but the fact that the gas and vapour have different velocities due to binary diffusion was retained by splitting the velocities into bulk and diffusive components :

$$\mathbf{v}_1 = \mathbf{v}_\gamma + \mathbf{u}_1 \quad (4)$$

$$\mathbf{v}_2 = \mathbf{v}_\gamma + \mathbf{u}_2. \quad (5)$$

Velocities \mathbf{u}_1 and \mathbf{u}_2 are due to the binary diffusion in the mixture.

2. If the temperatures of the various phases are unequal, energy will be transferred between phases. As discussed by Sheridan and Close [5], one of the possible explanations for the scatter when experimental values of Nu^* are plotted against Ra^* , as for example in Cheng [9], and Nu^{**} against Ra^{**} for the gas/vapour mixture [4], is because the terms in the equations resulting from the transfer between phases should be retained; normally they are neglected. In a continuum each point is by definition at a single state, so the 'state' at a point is dependent on the state of all of the four phases present. The transfer of energy between phases is really a boundary condition in the energy equation for that phase, but there are no boundaries in the continuum. This was resolved here by considering all interphase energy transfers to be source (or sink) terms. Assuming that

$$\dot{Q}_\sigma = (hA_v)_{\sigma\beta} (T_\beta - T_\sigma) \quad (6)$$

the energy equation for the solid can be written as

$$\rho_\sigma C_{p\sigma} \frac{\partial T_\sigma}{\partial t} = \nabla \cdot k_\sigma \nabla T_\sigma + (hA_v)_{\sigma\beta} (T_\beta - T_\sigma) \quad (7)$$

where A_v is the surface area per unit volume of the continuum. All transfers of energy between phases were introduced in this way.

3. The conservation of energy equation for the gas/vapour mixture is written as

$$\frac{\partial \sum_{i=1}^2 (\rho_i h_i)}{\partial t} + \sum_{i=1}^2 \nabla \cdot (\rho_i \mathbf{v}_i h_i) = -\nabla \cdot \mathbf{q}_\gamma + \dot{Q}_\gamma \quad (8)$$

where

$$\dot{Q}_\gamma = (hA_v)_{\beta\gamma} (T_\beta - T_\gamma) \quad (9)$$

and

$$\mathbf{q}_\gamma = -k_\gamma \nabla T_\gamma. \quad (10)$$

Using the conservation of mass to reduce the left-hand side of (8), this becomes

$$\begin{aligned} -\dot{m}_c h_1 + (\rho_1 C_{p1} + \rho_2 C_{p2}) \frac{\partial T_\gamma}{\partial t} + \mathbf{v}_\gamma \cdot (\rho_1 C_{p1} + \rho_2 C_{p2}) \\ \cdot \nabla T_\gamma + \rho_1 C_{p1} \mathbf{u}_1 \cdot \nabla T_\gamma + \rho_2 C_{p2} \mathbf{u}_2 \\ \cdot \nabla T_\gamma = \nabla \cdot k_\gamma \nabla T_\gamma + (hA_v)_{\beta\gamma} (T_\beta - T_\gamma). \end{aligned} \quad (11)$$

Assuming a weighted mixture specific heat

$$\rho_1 C_{p1} + \rho_2 C_{p2} = \rho_\gamma C_{p\gamma} \quad (12)$$

and with the binary diffusive mass flux given by

$$\mathbf{j} = \rho_1 \mathbf{u}_1 = -\rho_2 \mathbf{u}_2 \quad (13)$$

$$\begin{aligned} \rho_\gamma C_{p\gamma} \frac{DT_\gamma}{Dt} = \nabla \cdot k_\gamma \nabla T_\gamma + (hA_v)_{\beta\gamma} (T_\beta - T_\gamma) \\ + \dot{m}_c h_1 - \mathbf{j} \cdot (C_{p1} - C_{p2}) \nabla T_\gamma. \end{aligned} \quad (14)$$

The evaporation/condensation term in the equations describing conservation of energy for the liquid and gas/vapour phases must also be considered in light of the use of the continuum to represent all phases. Change of phase occurs at a boundary between phases and as such is a boundary condition. If the energy equations for the β and γ phases were added the resulting term would be $\dot{m}_c(h_\gamma - h_\beta)$, which is equivalent to $\dot{m}_c h_{fg}$. This would be the latent heat transfer at the phase interface and as such is the proper term when the equations are written in this form. An alternative and more correct approach—which produces the same result—is given by Whitaker [10] using the volume averaging approach as described by Whitaker and Slattery [7].

4. The momentum equation for the gas/vapour mixture,

$$\mathbf{v}_\gamma = -\frac{\kappa}{\mu}(\nabla p - \rho_\gamma \mathbf{g}), \quad (15)$$

can be written as a vorticity equation:

$$\zeta = -\frac{\kappa}{\mu}[\nabla \times \{\bar{\rho}_\gamma + \beta \bar{\rho}_\gamma(T - \bar{T}) + \beta_m \bar{\rho}_\gamma(m - \bar{m})\} \mathbf{g}] \quad (16)$$

where the thermal and mass expansion coefficients are defined as

$$\beta = \frac{1}{V} \left(\frac{\partial V}{\partial T} \right)_{p,m} = -\frac{1}{\rho} \left(\frac{\partial \rho}{\partial T} \right)_{p,m} \Big|_T \quad (17)$$

and

$$\beta_m = \frac{1}{V} \left(\frac{\partial V}{\partial m} \right)_{p,T} = -\frac{1}{\rho} \left(\frac{\partial \rho}{\partial m} \right)_{p,T} \Big|_{\bar{m}} \quad (18)$$

2.2. Non-dimensional form of the equations

The conservation equations developed above were put in non-dimensional form using Kline's approach [11]. This entails using reference variables which result in non-dimensional variables in the range 0 to 1. The choice of the appropriate reference variable is not always straightforward and in natural convection the choice of non-dimensional time and velocity is a point of some discussion.

Table 1 shows the form of non-dimensional variables used here, where

$$\Delta m_s = m_{\text{hot},s} - m_{\text{cold},s}$$

The resulting dimensionless equations, in two-dimen-

sional form, are listed below. In the following equations variables T , m , v , x and t are now dimensionless.

2.2.1. *Momentum equation for the gas/vapour mixture.* Letting x_3 be parallel to the gravity vector and defining an aspect ratio $A = H/L$, equation (15) becomes

$$\frac{\partial v_1}{\partial x_3} - A \frac{\partial v_3}{\partial x_1} = A \left[Ra^* \frac{\partial T}{\partial x_1} + Ra_m^* \frac{\partial m}{\partial x_1} \right] \quad (19)$$

where v_1 and v_3 are the velocity components in directions x_1 and x_3 respectively, and

$$Ra^* = \frac{\kappa \rho_\gamma C_{p\gamma} H \beta \Delta T g}{\nu k^*}$$

$$= Ra Da$$

$$Ra_m^* = \frac{\kappa \rho_\gamma C_{p\gamma} H \beta_m \Delta m g}{\nu k^*}$$

Equation (19) can be written as

$$\frac{\partial v_1}{\partial x_3} - A \frac{\partial v_3}{\partial x_1} = A Ra Da \left[\frac{\partial T}{\partial x_1} + N \frac{\partial m}{\partial x_1} \right] \quad (20)$$

where

$$N = (\beta_m \Delta m / \beta \Delta T)$$

and for a perfect gas,

$$\beta_m = \left[\frac{M_2 - M_1}{(1+m)(M_1 + mM_2)} \right]. \quad (21)$$

2.2.2. *Energy equation for the liquid.* Assuming

$$\dot{m}_c = (h_d A_\nu)_{\beta_\gamma} (m - m_{s\beta}) \quad (22)$$

where $m_{s\beta}$ = saturated mass fraction at T_β and m = actual mass fraction in gas/vapour mixture and with

$$\frac{hH}{k} = a Re^b Pr^c \quad (23)$$

$$\frac{h_d H}{\rho D} = a Re^b Sc^c \quad (24)$$

from Eckert and Drake [12] one can obtain a relationship between the heat and mass transfer coefficients:

$$\frac{h}{h_d C_p} = (Le)^{1-c}. \quad (25)$$

Using this and the definition of the Jakob number,

$$Ja = \frac{C_p \Delta T}{\Delta m h_{fg}}, \quad (26)$$

the dimensionless form of the energy equation for the liquid is

$$\frac{\partial T_\beta}{\partial t} = \left(\frac{\alpha_\beta}{\alpha^*} \right) \left\{ A^2 \frac{\partial^2 T_\beta}{\partial x_1^2} + \frac{\partial^2 T_\beta}{\partial x_3^2} + Bi_{\sigma\beta} (T_\sigma - T_\beta) + Bi_{\beta\gamma} [(T_\gamma - T_\beta) + (Le)^{c-1} (Ja)^{-1} (m - m_{s\beta})] \right\} \quad (27)$$

where

Table 1. Non-dimensional variables

Variable	Non-dimensional form
Length	x_i/H
Temperature	$(T - T_{\text{cold}})/\Delta T$
Moisture content	$(m - m_{s,\text{cold}})/\Delta m_s$
Velocity	$v/(k^*/\rho_\gamma C_{p\gamma} H)$
Time	$t/(H^2 \rho_\gamma C_{p\gamma}/k^*)$

$$Bi_{\beta\gamma} = \frac{(hA_v)_{\beta\gamma} H^2}{k_\beta} \quad \frac{\partial \rho_\gamma}{\partial x} = \frac{d\rho_\gamma}{dT} \frac{\partial T}{\partial x} \quad (30)$$

= an effective Biot number. (28)

2.2.3. Energy equation of the gas/vapour mixture. Using the same approach equation (14) becomes

$$\frac{\partial T_\gamma}{\partial t} = \left(\frac{\alpha_\gamma}{\alpha^*} \right) \left\{ A^2 \frac{\partial^2 T_\gamma}{\partial x_1^2} + \frac{\partial^2 T_\gamma}{\partial x_3^2} + Bi_{\beta\gamma} (T_\beta - T_\gamma) (Le)^{c-1} (Ja)^{-1} (m - m_{s\beta}) \right\}. \quad (29)$$

The sensible heat transfer by binary diffusion, due to the difference in specific heats of the gas and vapour, has been eliminated using an argument based on scaling and their relative orders of magnitude. This argument is valid for most cases, including the air/water case being considered here, but there may be some combinations of gases and vapours where its validity needs further examination.

The set of dimensionless variables for the parametric model is shown in Table 2. Not all of these can be extracted directly from the experimental data. For example, the Biot numbers require a value for the local heat transfer coefficient between phases. This will be obtained using the relationship between heat transfer coefficient and Prandtl number—and in the case of mass transfer the Lewis or Schmidt number.

2.3. Analogy model

The derivation of what is referred to as the analogy model is based on the original work of Close [3] and the extension of this to heat and mass transfer in open cavities by Close and Sheridan [2]. It is fully described by Sheridan [8].

A volume expansion coefficient for this case is derived assuming the perfect gas and Clausius–Clapeyron relationships. This means the density can be written as a function of temperature only, rather than as a function of temperature and mass fraction. Hence,

$$\rho_\gamma = \frac{p}{RT} \left[\frac{(1+m)M_1 M_2}{(M_1 + mM_2)} \right] \quad (31)$$

and

$$\frac{d\rho_\gamma}{dT} = \frac{(M_1 - M_2)}{RT^2} \frac{dp_1}{dT} - \rho_\gamma/T. \quad (32)$$

Using the Clausius–Clapeyron relationship the momentum equation becomes

$$\zeta = -\frac{\kappa}{\mu} g \beta' \rho_\gamma \frac{\partial T}{\partial x_1}. \quad (33)$$

The energy equation is written with

$$T_\sigma = T_\beta = T_\gamma,$$

giving

$$\nabla \cdot (\rho_2 \mathbf{v}_\gamma h_\gamma) + \nabla \cdot \mathbf{j} h_1 - \nabla \cdot \mathbf{j} h_2 + \nabla \cdot (\rho_\beta \mathbf{v}_\beta h_\beta) = \nabla \cdot (k^* \nabla T) \quad (34)$$

where h_γ has been defined per unit mass of the inert gas.

From the conservation of mass of the vapour and liquid,

$$\nabla \cdot (\rho_\beta \mathbf{v}_\beta) = \nabla \cdot \left[\rho_\gamma D \nabla \left(\frac{m}{1+m} \right) \right] - m \nabla \cdot (\rho_2 \mathbf{v}_\gamma) - \rho_2 \mathbf{v}_\gamma \cdot \nabla m, \quad (35)$$

the energy equation becomes

$$h_\gamma \nabla \cdot (\rho_2 \mathbf{v}_\gamma) + \rho_2 \mathbf{v}_\gamma \cdot \nabla h_\gamma + \rho_\beta \mathbf{v}_\beta \cdot \nabla h_\beta + h_\beta \left\{ \nabla \cdot \rho_\gamma D \nabla \left(\frac{m}{1+m} \right) - m \nabla \cdot \rho_2 \mathbf{v}_\gamma - \rho_2 \mathbf{v}_\gamma \cdot \nabla m \right\} = \nabla \cdot (k^* \nabla T) - \nabla \cdot \{ \mathbf{j} (h_1 - h_2) \} \quad (36)$$

where in equation (30) it has been assumed that the

Table 2. Non-dimensional numbers for parametric model

Dimensionless number	Equation	Significance
Ra	$g\beta\Delta TH^3/\alpha\nu$	The ratio of buoyancy to viscous forces in a fluid layer
Da	κ/H^2	Accounts for the effect of geometry of the porous medium on the fluid flow
N	$\beta_m \Delta m / \beta \Delta T$	Measures the significance of the contribution to buoyancy of the variation in vapour concentration
Ja	$C_p \Delta T / \Delta m h_{fg}$	The ratio of sensible heat transfer potential to latent heat transfer potential
Le	α/D	Is a measure, with the Prandtl number, of the interphase mass transfer
A	H/L	The aspect ratio
Pr	ν/α	Affects two factors. (i) The interphase heat transfer and (ii) the inertial forces contribution (see Sheridan [13])

vapour concentration is a function only of temperature, as it is saturated, that is

$$m = m(T)$$

then

$$\nabla m = \frac{dm}{dT} \nabla T.$$

Using this and the following result from the conservation of mass,

$$\nabla \cdot (\rho_2 \mathbf{v}_\gamma) = -\nabla \rho_\gamma D \nabla \left(\frac{m}{1+m} \right), \quad (37)$$

gives

$$\begin{aligned} & -\rho_\gamma D \nabla \left(\frac{m}{1+m} \right) \{h_\gamma - mh_\beta\} \\ & + \rho_2 \mathbf{v}_\gamma \left[\frac{d(h_\gamma + \Upsilon h_\beta)}{dT} - h_\beta \frac{dm}{dT} \right] \nabla T \\ & + h_\beta \left\{ \nabla \cdot \rho_\gamma D \frac{d}{dT} \left(\frac{m}{1+m} \right) \nabla T \right\} = \nabla \cdot (k^* \nabla T) \\ & - \nabla \cdot (\mathbf{j}[h_1 - h_2]) \end{aligned} \quad (38)$$

where

$$\Upsilon = \frac{\rho_\beta \mathbf{v}_\beta}{\rho_2 \mathbf{v}_\gamma} \text{ (a recirculation parameter).} \quad (39)$$

Grouping advective and diffusive terms gives

$$\begin{aligned} & \rho_2 \mathbf{v}_\gamma \left[\frac{d(h_\gamma + \Upsilon h_\beta)}{dT} - h_\beta \frac{dm}{dT} \right] \nabla T = \nabla \cdot (k^* \nabla T) \\ & + \nabla \cdot \left\{ \rho_\gamma D \frac{d}{dT} \left(\frac{m}{1+m} \right) \nabla T \right\} \{h_2 + mh_1 - mh_\beta - h_\beta\} \\ & + \nabla \cdot \left\{ \rho_\gamma D \frac{d}{dT} \left(\frac{m}{1+m} \right) \nabla T \right\} (h_1 - h_2). \end{aligned} \quad (40)$$

This can be written as

$$\rho_2 \mathbf{v}_\gamma C^* \nabla T = \nabla \cdot (k^{**} \nabla T) \quad (41)$$

where

$$C^* = \frac{d(h_\gamma + \Upsilon h_\beta)}{dT} - h_\beta \frac{dm}{dT} \quad (42)$$

and

$$k^{**} = k^* + \rho_\gamma D (1+m) h_{\text{fg}} \frac{d}{dT} \left(\frac{m}{1+m} \right). \quad (43)$$

This equation is put in non-dimensional form using the variables given in Table 1, with the exception that

the effective thermal diffusivity $\alpha^{**} = k^{**}/(\rho_2 C^*)$ is used in making the velocity and time dimensionless.

This gives the final form of the non-dimensional energy equation:

$$\mathbf{v}_\gamma \cdot \nabla T = \nabla^2 T. \quad (44)$$

The momentum equation becomes

$$\zeta = Ra^{**} \frac{\partial T}{\partial x_1} \mathbf{x}_2 \quad (45)$$

where

$$Ra^{**} = \frac{\kappa \beta' \Delta T H g}{\alpha^{**} \nu} \quad (46)$$

and the aspect ratios are the only dimensionless parameters for this model. (It should be noted that the non-linear term discussed by Close and Sheridan [2] has been neglected in deriving the final form of the equations.)

The preliminary parametric study [5] indicated that neither Pr nor Le played a significant role in the experiments reported in ref. [4]. Since these parameters are primarily concerned with transfer between fluid and packing, the results suggest that the rate coefficients are high enough for the mixture to be at or near saturation. This view is supported by the reasonable success of the simple analogy model in correlating the data in ref. [4].

Of the remaining parameters it is obvious that from the physics of the problem and the results presented in ref. [5], Ra , Da , Ja and N play a critical role in the system behaviour.

3. EXPERIMENTAL APPARATUS AND METHOD

The experiments described were aimed at testing the following hypotheses:

(a) The physical process is one in which the convective heat and mass transfer has an analogous form to that for heat transfer only. As a consequence, it is postulated that a model based on this analogy can be used to describe the process.

(b) This analogy model is applicable over the range of temperature differences across the bed which might be used in practice.

(c) The analogy model can be applied to beds of different geometries.

(d) An alternative model, based on dimensionless variables resulting from a parametric analysis, is a better predictor of heat transfer than the analogy model.

Sheridan [8] discusses these in more detail. He also presents further experimental results where temperatures in the bed were measured during steady-state and transient operating conditions. The only other experimental data that appear to have been published on this process are those of Close and Peck

Table 3. Ranges of derived independent variables

Variable	Maximum	Minimum	Uncertainty
Measured			
T_{hot}	65	40	0.02
T_{cold}	62.5	20	0.02
ΔT	40	2.5	0.02
\bar{T}	63.75	30	0.02
Derived			
Ra	1.3×10^8	7.09×10^6	0.08
Da	2.44×10^{-5}	2.4×10^{-5}	0.08
N	1.44	0.3	0.12
Ja	0.28	0.05	0.08
Le	0.81	0.65	0.05
Pr	0.92	0.74	0.05
Ra^{**}	14013	891	0.19

[4] (hereafter referred to as CP). Their experiments were planned with the objective of establishing the viability of the process for technological applications. The study described here was concerned both with the question of how much heat is transferred for a given set of independent variables, and how heat is transferred through the bed, i.e. what are the important transport mechanisms?

It was recognized that, because of the number of transport phenomena involved, this study could not answer all the questions of interest. In selecting the independent variables to be examined the requirements of an engineer using the process to design a thermal component were considered. From that perspective the effect of the following three factors are of interest:

- The operating temperatures of the source and sink.
- The geometry of the bed and its boundaries.
- The gas and vapour used.

The experimental facility was designed such that all of these could be varied over a wide range. Only the effect of temperature was specifically tested in the experiments described here. The range of the variables examined and their uncertainties, as defined by Kline and McClintock [14], are given in Table 3. The uncertainties are all at the 20:1 odds level; those for the measured variables were estimated from the calibrations and design calculations while those of the derived variables were obtained using the method outlined in Kline and McClintock's paper.

The apparatus used is shown in Fig. 2. The test bed is housed in a box which is sealed at the top and bottom by isothermal plates, and whose walls are guard heated to approximate adiabatic conditions.

Complete details of the equipment are given by Sheridan [8], so only a brief description will be given here.

The isothermal plates, shown in Fig. 3, comprised an electrically heated aluminium plate in contact with the bed and a water heated plate acting as a guard. Heat flux meters between these plates allowed the

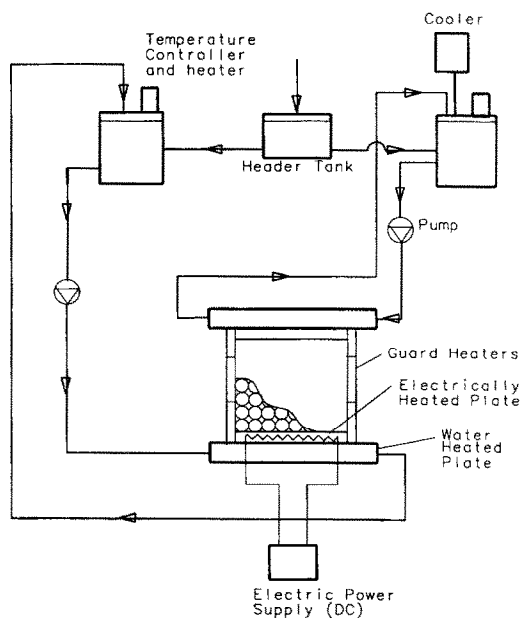


Fig. 2. Schematic of the experimental apparatus.

power to the inner plate to be adjusted so negligible heat was transferred from it to the surroundings. Lateral heat losses from the electrically heated plates were minimized using a guard heater around its edges.

The temperatures of each of the electrically heated plates were measured by five thermocouples located in a star pattern, with their junctions within 1 mm of the surface. The thermocouple leads passed through holes drilled in the water heated plates. Of the five thermocouples, two measured the plate temperature, while the other three were connected to three in the other plate to measure the temperature difference between the plates.

The walls of the bed were made of stainless steel to minimize conduction. They were guard heated, each guard being 110 mm high, further insulated with 100 mm of mineral wool insulation, and to further minimize effects from fluctuating ambient conditions, the apparatus was enclosed by a box made of 75 mm-thick polystyrene sheet.

The packing comprised table tennis balls, each filled with polyurethane foam. The balls were packed in a $9 \times 9 \times 9$ face oriented array, i.e. the least dense packing arrangement. Fine thermocouples were placed in 81 of them to measure the temperature distribution of the bed during operation.

Most of the experiments were performed at steady-state conditions. These were achieved by setting the plate temperatures using the water bath controllers, and adjusting the power supply to the electrically heated plates to null the heat flux meter readings. As an exact null was not achievable, the criterion used was that the heat flux meters read less than 5% of the power input for longer than 2 h. Generally, steady-state was reached after 18–20 h.

Because conduction was considered more stable

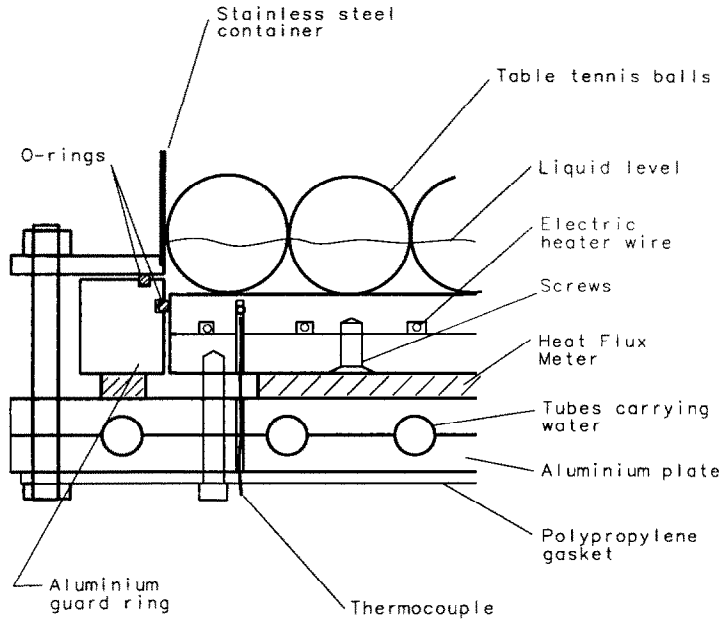


FIG. 3. Detail of the heated isothermal plates.

than convection and because estimates of conductivity are inherently more reliable than those of Nusselt number, conduction was chosen as the primary heat transfer mechanism for calibrating the heat flux measurement.

These calibration measurements were made using as the sample a layer of gas 11 mm high. The side walls were made from balsa wood with a reflective foil coating facing the gas layer. Other than this, the plates and instrumentation were identical to the final experimental arrangement. During the calibration runs the thermocouples in the plates were found to reliably measure within 0.1 K of each other (having been found previously to read to this accuracy by comparison with a reference standard) and to vary by less than 0.2 K over a period of 2 h. Measurements of heat flux were made with three gases: helium, air and Freon-12. Estimates of the thermal conductivity based on the measurements made were in good agreement with reference values.

For the same arrangement, the natural convection in a plane, horizontal layer of large aspect ratio was measured and compared with the results and correlation of Raithby and Hollands [15]. These measurements were made around the critical Rayleigh number and showed good agreement both with the values of Nusselt number predicted by the correlation and their measurement of the critical Rayleigh number.

4. RESULTS AND DISCUSSION

Heat transfer rates through the bed as a function of mean temperature and temperature difference are shown in Fig. 4.

The increase in heat transfer with mean temperature

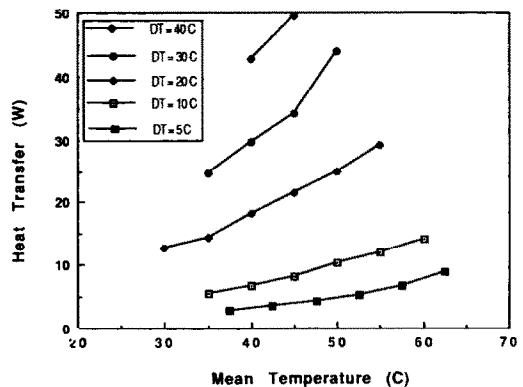


FIG. 4. Heat transfer variation with mean bed temperature.

is due to the presence of the water. As the temperature is increased the curvature of the vapour pressure vs temperature curve results in larger differences in moisture content for a constant temperature difference. This increases the density difference across the bed resulting in a larger buoyancy force and, hence, velocity. It also increases the potential for evaporation and condensation resulting in a greater transfer of latent heat.

Figure 5 combines the current experimental results with those of Close and Peck [4] and those obtained for the analogous heat transfer case, as presented by Cheng [9]. The so-called analogy model developed above results in equations for the conservation of momentum and energy which have the same dimensionless form for the heat and mass transfer case as those for the equivalent heat transfer case. Only the

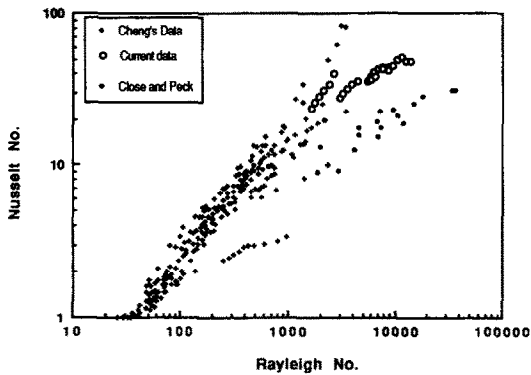


FIG. 5. Experimental results for heat and mass transfer case combined with results for the heat transfer case as collated by Cheng [9].

dimensionless parameters are different. Thus, if the assumptions made in developing the model, as detailed above, are valid, there should be a direct correspondence between the relationships between Nu^* and Ra^* and Nu^{**} and Ra^{**} . Figure 5 allows this to be tested.

There is good agreement between the current experimental results for heat and mass transfer with those for heat transfer. The importance of this is not only in the evidence for the validity of the analogy model but also in the similarity between the dominant mechanisms by which heat is transferred in the two cases. In particular, it implies that the temperature field is of primary importance in determining the physics of the heat and mass transfer case even though the heat transferred is increased by the added buoyancy and latent heat transfer caused by the presence of the volatile component. Results from the different heat transfer studies (represented by different symbols on the graph) collated by Cheng show a wide band of scatter, the possible causes of which have been discussed by Sheridan *et al.* [16]. The current results are clustered together in groups having the same ΔT .

Two possible ways in which ΔT could affect the relationship between Nu^{**} and Ra^{**} are:

(a) by introducing non-linearities through property variations;

(b) by invalidating some aspect of the analogy model development. For example, some transport phenomenon which was important had not been considered in the model development. An example of such a phenomenon, which was determined not to be relevant in the present study but could be if the particle size were reduced, is the capillary transfer of liquid in the bed. Alternatively, the assumptions made could depend on the magnitude of the temperature difference. Close and Sheridan [2] discuss such a case for the open cavity case, where they show that there is a non-linear term in the dimensionless equations, caused by the form of k^{**} , which can only be neglected

below certain temperature differences and thus restricts the applicability of the analogy model.

A further conclusion to be drawn from Fig. 5 is that the relationship between the experimental values of Nu^{**} and Ra^{**} appears to be consistent for different values of ΔT and \bar{T} . One of the experimental objectives had been to examine the validity of the analogy model over a wider range of conditions than had been done previously. From Fig. 5 it would appear that for a wide range of temperatures the heat transfer (Nu^{**}) depends primarily on Ra^{**} with some dependence on ΔT and \bar{T} . Thus, the assumptions made in developing the model appear reasonable.

The effect of property variations on the analogy model was studied numerically [8]. This showed that these variations had a significant effect on the heat transfer correlation of Nu^{**} vs Ra^{**} and also on the critical Rayleigh number, Ra^{**} , at which convection starts. However, the effects were found not to be significant over the range of ΔT examined in the experiments. While the effect was similar in that Nu^{**} was lower for the same Ra^{**} when ΔT was higher, the magnitude in the experimental results was of a similar order when ΔT changed from 20 to 30 K as it was in changing from 0 to 30 K in the numerical model. In fact the numerical study showed that it was better to account for the effect of property variations by normalizing Ra^{**} with respect to the critical value than attempting to account for it by examining the effect on Nu^{**} for a particular Ra^{**} , i.e. the Nu^{**} vs Ra^{**} results for different ΔT are better matched by a horizontal 'shift' or normalization than a vertical one. As discussed by Sheridan *et al.* [16], ΔT has an effect on the property variation; the level of this effect depends on \bar{T} . This is caused by the curvature of the vapour pressure line and results in a non-linear variation of properties, such as k^{**} and C^* , with temperature. Thus the properties vary more for $\Delta T = 10$ K at $\bar{T} = 80^\circ\text{C}$ than they do at $\bar{T} = 30^\circ\text{C}$. The two factors, \bar{T} and ΔT , are thus both involved in the effect on property variations and affect the Nu^{**} vs Ra^{**} relationship in the following way. At a particular ΔT the data increase regularly with Ra^{**} (or mean temperature) with a slight degree of curvature. Assuming that the variation between data at different ΔT could be removed using ΔT , and the curvature removed by multiplying this by $\bar{T}^{0.25}$. Figure 6 shows the result of this manipulation. The data now all lie on a single line. This means a relationship of the form

$$Nu^{**}(\Delta T)\bar{T}^{0.25} \propto (Ra^{**})^n$$

would result in a good fit to the data.

It is not suggested that such a fit has been proved general at this stage and so it is not proposed as a universal modifier to the analogy model. What is important is the significance of the modification due

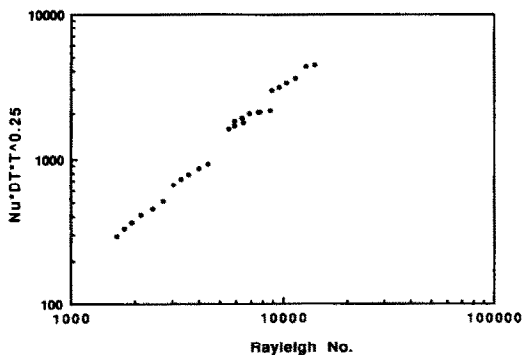


FIG. 6. Effect of ΔT and \bar{T} on the relationship between Nu^{**} and Ra^{**} .

to ΔT and \bar{T} , and the way it relates to the two possible effects of ΔT on Nu^{**} suggested originally.

All experiments described here were done with the same geometry. The effect of changes in geometry was examined by comparing these data with those of CP. The differences between the two sets of experiments are set out below.

(a) Cubic packing was used in this experiment; this is the least dense packing arrangement with a calculated porosity of 0.4764. CP used rhombohedral packing; this is the densest packing arrangement with a calculated porosity of 0.2596.

(b) The table tennis balls used here had a mean diameter of 38 mm compared to 29 mm for the glass marbles used by CP. In combination these two differences result in permeabilities of 1.8×10^{-7} for CP and 3.8×10^{-6} here. The Darcy number varies by a similar ratio. The analogy model accounts for almost all geometrical effects through the permeability parameter. This is usually the case with models of transport phenomena in porous media. Thus, the geometry variation between the two sets of experiments is considered large enough to show effects attributable to geometry.

(c) The solid conductivity, which is included in the effective thermal conductivity, k^* , varied from $1.05 \text{ W m}^{-1} \text{ K}^{-1}$ for glass to $0.03 \text{ W m}^{-1} \text{ K}^{-1}$ for the polyurethane filled table tennis balls used here.

One other geometrical parameter exists in the analogy model. This is the tortuosity, defined as the ratio of the effective diffusivity of the gas and vapour in the porous medium to the diffusivity in a gaseous mixture. CP assumed a porosity of 0.2. One suggested way of calculating the tortuosity is the ratio of the flow path length to the sample length all squared:

$$\tau = (L/L_e)^2.$$

Bear [17] quotes a range of values for τ from the literature of

$$0.56 \leq L/L_e \leq 0.8$$

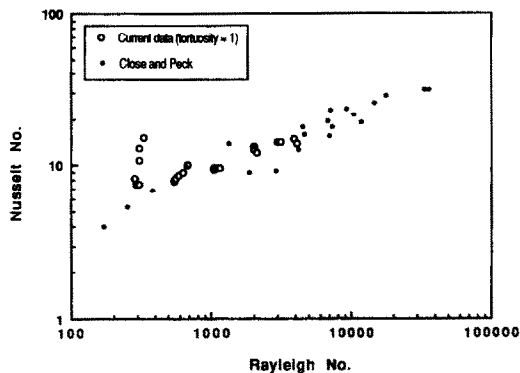


FIG. 7. Experimental results from this study with a tortuosity of 1.0 compared to those of Close and Peck [4] with a tortuosity of 0.2.

corresponding to

$$0.31 \leq \tau \leq 0.64,$$

with a value of $\frac{1}{3}$ for an isotropic medium, such as that of CP. These values are generally empirically derived, and while attempts are made to relate them to porosity or permeability no definitive relationship appears to have been found. Bear states that the relationship between permeability and tortuosity is of the form

$$\kappa = \epsilon \tau B$$

where B is the 'hydraulic conductance' of the medium and is related to the shape of the channels through which the fluid flows. Given the difference between the two permeabilities, this suggests that the tortuosities would also be significantly different between the two cases. Two tortuosities were used here, 0.2 and 1.0, the latter being an upper limit.

Figures 5 and 7 show the results from the present study with those of CP. Considering CP's data are for air/water only, the current data with $\tau = 0.2$ are about 20% higher than an extrapolation of their data to $Ra^{**} = 3000$. When $\tau = 1$ the current data are 12% lower than CP's at $Ra^{**} = 3000$. Considering the very large differences in the geometrical variables the agreement is good, but the effect of geometry needs further investigation. The data presented here are insufficient on which to base a modification to the analogy model to account for geometry. However, from the agreement between the two data sets and the variation of Nu^{**} vs Ra^{**} with τ , it appears that such a modification, based on the permeability and particle diameter or the tortuosity, might be found. The parametric model of this process developed above was used to identify the important dimensionless parameters (listed in Table 2) for this process.

The Nusselt number based on fluid properties, Nu_f , was correlated against these independent variables. Fluid properties were used in the Nusselt number because using the mixture conductivity, rather than k^* or k^{**} , removes any argument concerning the appropriate model for thermal conductivity in a packed bed. This is done at the expense of using a

possibly unrealistic conductivity at low Rayleigh numbers, where conduction through the solid may become important. In these experiments this regime was not tested. Also, the conductivity of the solid was not dissimilar to that of the fluid.

The data were correlated using multivariate regression as described by Sheridan and Close [5]. As found previously, the variables against which Nu_f correlated best were those governing the buoyancy, Ra , Da and N , and the Jakob number, Ja , which is the ratio of sensible to latent heat transfer potentials.

The fit found by Sheridan and Close was

$$Nu_f \propto (Ra Da N)^{0.295} Ja^{-0.45}$$

This was also found to fit the experimental data from this study. While the exponents on the dimensionless groups fitted both sets of data well, the coefficients of proportionality were very different. The lines of best fit for the two data sets were

(a) Current data

$$Nu_f = 6.66(Ra Da N)^{0.295} Ja^{-0.45}$$

(b) Close and Peck

$$Nu_f = 0.54(Ra Da N)^{0.295} Ja^{-0.45}$$

Figure 8 plots the Nusselt number predicted by these correlations against the measured values. In general, the agreement is good given the uncertainties associated with the independent variables listed in Table 3. The uncertainty associated with the Nusselt number depends on the heat being transferred through the sample, i.e. it is a function of the Nusselt number itself. This is because the major source of error in Nusselt number is caused by losses from the 'box' to ambient. These losses depend on \bar{T} and are proportionally much higher for the case where the hot plate surface is at 65°C and the cold at 60°C than when the hot plate is at 65°C and the cold at 20°C. The relative uncertainties, at the 20:1 odds level, are 0.43 and 0.09 respectively for these cases.

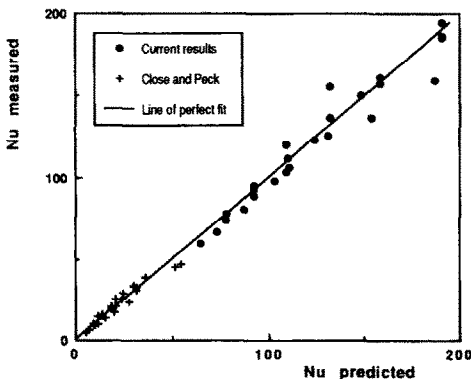


FIG. 8. Prediction of Nusselt number using the parametric model.

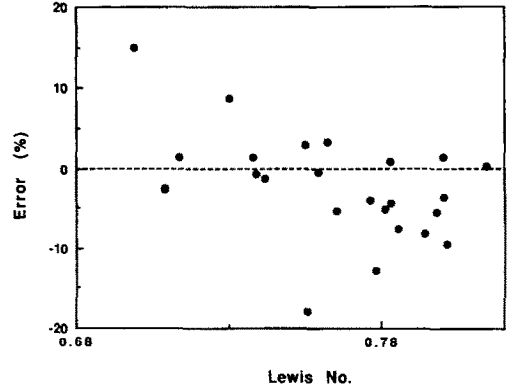


FIG. 9. Correlation between Lewis number and the residuals from the prediction of the Nusselt number by the parametric model.

It seems likely that the cause of the difference between the two correlations is the difference in geometry between the two samples, as discussed above. To confirm this, and to determine which geometrical parameter characterizes the effect, requires more data be taken with different geometries.

The two most important dimensionless variables in predicting heat transfer are the ratio of buoyancies, N , and the Jakob number, Ja . These are both strongly correlated with the difference in mass fraction across the bed, and in that sense are also cross-correlated. This does not mean, however, that only one of them is the primary dimensionless variable. Nu_f was predicted more accurately using both N and Ja than when either was used on its own. As noted in Table 2, they are indicators of different effects. The fact that both are important means that the latent heat transfer is important (Ja) but convective movement is needed (N) to transport the vapour between its source and sink.

Figures 9 and 10 show the residuals from the prediction of Nu_f using the above relationship plotted against the Lewis (Le) and Prandtl (Pr) numbers.

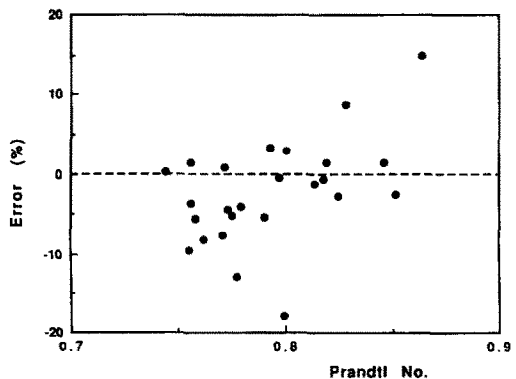


FIG. 10. Correlation between Prandtl number and the residuals from the prediction of the Nusselt number by the parametric model.

These were expected to be important if the heat transfer was affected by the rate at which heat and mass were transferred between the solid surfaces or particles and the fluid. Judging from these figures, the rate processes are not significant in overall heat transfer. The narrow range of Le and Pr should be noted, and while these variables would not be expected to vary a great deal for most gas/vapour mixtures they may have more influence in some other cases where the geometry and thermal conductivity of packing material are different.

On the basis of these results, however, the assumption of infinite rate coefficients made in deriving the analogy model appears reasonable.

5. CONCLUSIONS

From the results presented the following conclusions can be drawn.

(a) The model based on the analogy between heat and mass transfer can be used to correlate the experimental data, but several factors suggest the actual transport processes transferring heat operate differently from the way previously assumed.

(b) The temperature difference across the bed has an effect beyond that accounted for in the analogy model. This was shown in the Nu^{**} vs Ra^{**} graphs presented. The experimental data show a greater effect due to ΔT than found to be due to property variations by a numerical study. Also, the fact that the parametric model, where buoyancy and latent heat effects are separated, correlates the data better suggests that the analogy model is restricted by its lumping or combining of these effects.

(c) While the examination of geometrical effects was limited to a comparison of the results from the present study with those of Close and Peck [4], there appears to be an effect due to geometry beyond that accounted for in the models by the permeability parameter. In the analogy model the tortuosity factor may account for this but further work is needed to quantify the effect.

(d) The data are better correlated by the parametric model than the analogy model. This appears to be due to the differentiation of the effects due to convection and latent heat transfer, through the buoyancy ratio and the Jakob number, compared to the lumped parameter approach of the analogy model.

This work examines a physical process which,

somewhat surprisingly, has only been examined in a limited way previously. Much remains to be done in fully determining the interaction of the many separate transport processes involved; the models and experimental results presented herein hopefully provide a useful base on which to build.

REFERENCES

1. D. J. Close and M. K. Peck, High temperature thermal energy storage: a method of achieving rapid charge and discharge, *Solar Energy* **37**, 269–278 (1986).
2. D. J. Close and J. Sheridan, Natural convection in enclosures filled with a vapour and a non-condensing gas, *Int. J. Heat Mass Transfer* **32**, 855–862 (1989).
3. D. J. Close, Natural convection with coupled mass transfer in porous media, *Int. Commun. Heat Mass Transfer* **10**, 465–476 (1983).
4. D. J. Close and M. K. Peck, Experimental determination of the behaviour of wet porous beds in which natural convection occurs, *Int. J. Heat Mass Transfer* **29**, 1531–1541 (1986).
5. J. Sheridan and D. J. Close, Transfer mechanisms governing natural convection in porous media with coupled mass transfer, *Proc. 2nd ASME/JSME Thermal Engineering Conf.*, Honolulu (1987).
6. R. B. Bird, W. E. Stewart and E. N. Lightfoot, *Transport Phenomena*. Wiley, New York (1960).
7. J. C. Slattery, *Momentum, Energy and Mass Transfer*. McGraw-Hill, New York (1972).
8. J. Sheridan, Natural convection with coupled heat and mass transfer in porous media, Ph.D. Thesis, Monash University, Melbourne (1989).
9. P. Cheng, Heat transfer in geothermal systems, *Adv. Heat Transfer* **14**, 1–105 (1979).
10. S. Whitaker, Simultaneous heat, mass and momentum transfer in porous media: a theory of drying, *Adv. Heat Transfer* **13**, 119–203 (1977).
11. S. J. Kline, *Similitude and Approximation Theory*. McGraw-Hill, New York (1965).
12. E. R. G. Eckert and R. M. Drake, *Introduction to the Transfer of Heat and Mass*. McGraw-Hill, New York (1959).
13. J. Sheridan, The influence of inertial forces on natural convection through a horizontal porous layer. CSIRO Div. Energy Tech. Report DET 87/35 (1987).
14. S. J. Kline and F. A. McClintock, Describing uncertainties in single sample experiments, *Mech. Engng* **75**, 3–8 (1953).
15. G. D. Raithby and K. G. T. Hollands, Natural convection. In *Handbook of Heat Transfer: Fundamentals* (Edited by W. M. Rohsenow *et al.*), Chap. 6. McGraw-Hill, New York (1985).
16. J. Sheridan, A. Williams and D. J. Close, The effect of transport properties on heat and mass transfer in porous media, *Proc. Fourth Australasian Conf. on Heat and Mass Transfer*, Christchurch (1989).
17. J. Bear, *Dynamics of Fluids in Porous Media*. American Elsevier, New York (1972).

ETUDE EXPERIMENTALE DE CONVECTION NATURELLE DE TRANSFERT DE CHALEUR ET DE MASSE DANS LES MILIEUX POREUX

Résumé—On examine les transferts couplés de chaleur et de masse dans les milieux poreux où la convection naturelle est provoquée par des différences de température et de concentration. Deux modèles non dimensionnels concurrents sont développés pour représenter le transfert thermique mesuré expérimentalement à travers un milieu poreux. On montre qu'un modèle paramétrique corrèle bien les données avec une forme générale $Nu \propto (Ra Da N)^{0.295} Ja^{-0.45}$. L'autre modèle, basé sur l'analogie entre transferts de chaleur et de masse, est moins précis dans la prédiction du transfert de chaleur mais les résultats sont assez bons pour suggérer que de tels modèles analogiques peuvent être utilisés dans un large domaine de mécanismes de transfert de chaleur et de masse. On discute aussi l'effet de la géométrie de lit pour les deux modèles.

EXPERIMENTELLE UNTERSUCHUNG DER NATÜRLICHEN KONVEKTION BEI
GEKOPPELTEM WÄRME- UND STOFFTRANSPORT IN PORÖSEN MEDIEN

Zusammenfassung—In der vorliegenden Arbeit wird der gekoppelte Wärme- und Stofftransport in porösen Medien bei thermisch- und konzentrationsgetriebener natürlicher Konvektion untersucht. Zwei verschiedene dimensionslose Modelle werden entwickelt. Mit ihrer Hilfe werden die Versuchsergebnisse für den Wärmetransport in einem porösen Medium korreliert. Es zeigt sich, daß ein parametrisches Modell der folgenden Form gut für die Korrelation geeignet ist: $Nu \propto (Ra Da N)^{0,295} Ja^{-0,45}$. Das andere Modell, das auf der Analogie von Wärme- und Stoffübertragung beruht, beschreibt den Wärmetransport weniger genau. Die Ergebnisse sind aber gut genug um vorzuschlagen, daß solche Analogiemodelle in einem weiten Bereich des Wärme- und Stofftransports eingesetzt werden können. Außerdem wird der Einfluß der Bettgeometrie auf die beiden Modelle diskutiert.

ЭКСПЕРИМЕНТАЛЬНОЕ ИССЛЕДОВАНИЕ ЕСТЕСТВЕННОЙ КОНВЕКЦИИ ПРИ
ВЗАИМОСВЯЗАННОМ ТЕПЛО- И МАССОПЕРЕНОСЕ В ПОРИСТЫХ СРЕДАХ

Аннотация—Исследуется взаимосвязанный тепло- и массоперенос в пористых средах с естественной конвекцией, обусловленной разностями температур и концентраций. Разработаны две альтернативные безразмерные модели, используемые для корреляции экспериментально измеренного потока тепла через пористую среду. Показано, что параметрическая модель хорошо обобщает полученные данные:

$$Nu \propto (Ra Da N)^{0,295} Ja^{-0,45}.$$

На основе аналогии между тепло- и массопереносом вторая модель менее точно рассчитывает процесс теплопереноса, однако полученные результаты свидетельствуют о том, что подобные модели могут применяться в широком диапазоне процессов тепло- и массопереноса. Обсуждается также влияние геометрии слоев на эффективность обеих моделей.